

A contribution to the modeling of permanent deformations of bituminous mixes

B. Dongmo-Engeland

SINTEF Technology and Society, Road and Railway Engineering, 7465 Trondheim, Norway.

Formerly: Département Génie Civil et Bâtiment (URA CNRS 1652), Ecole Nationale des TPE

H. Di Benedetto

Département Génie Civil et Bâtiment (URA CNRS 1652), Ecole Nationale des TPE, 6 Rue Maurice AUDIN, 69518 Vaulx en Velin, France.

ABSTRACT: Rutting is one of the well-recognized road surface distresses in asphalt concrete pavements that can affect the pavement service life and traffic safety. The rutting phenomenon is linked with the permanent deformation accumulated after each cyclic loading due to the traffic. It is rather badly described by the traditional pavement analysis method. No rational approach is proposed to model this effect. A new test was developed at the “Département Génie Civil et Bâtiment” (DGCB) of the “Ecole Nationale des Travaux Publics de l’Etat” (ENTPE) to study permanent deformation of bituminous mixes. Experimental tests were carried out in order to contribute with the comprehension of the phenomena and the formulation of a law adapted for the rutting phenomenon modeling. A thermo-viscoplastic law has been developed at the DGCB for bituminous mixes during the last decade. This law introduces various experimental observations: general linear viscoelastic behaviour in the small strain range, non-linearity and viscoplastic flow. The aim of this paper is to widen the scope of this law by introducing permanent deformation in his formalism. Comparisons between the experimental value and the computed value of the slope of the secondary stage are presented for three temperatures (15°C, 25°C and 35°C), two frequencies (1Hz and 10Hz), and five stress amplitudes (0.1MPa, 0.2MPa and 0.3MPa in compression and -0.05 and -0.1MPa in extension).

KEY WORDS: Bituminous mixes, rutting, rheological law, modeling, characterization, laboratory test.

1 INTRODUCTION

In order to study permanent deformation of bituminous mixes, a new test was developed at the “Département Génie Civil et Bâtiment” (DGCB) of the “Ecole Nationale des Travaux Publics de l’Etat” (ENTPE). This test provides direct information for the determination of the rheological law of the bituminous mixes. A unidimensional rheological model specifically developed at the DGCB for bituminous mixes is calibrated against the results of the test in order to simulate the accumulation of permanent deformation.

2 THE “T/C ENTPE” TEST

The principle of the T/C ENTPE test consists of applying an axial haversine stress to a cylindrical specimen. The permanent deformations which can reach some 10^{-2} m/m and the elastic deformation for each “small” cycle (around some 10^{-5} m/m) are measured in the same time (Di Benedetto, H. and Neifar, M., 2000), (Di Benedetto et al., 2003).

Data are proposed for a 0/14 bituminous mixes with pure 50/70 bitumen at 6.8 % by weight. Due to the lack of place only some results of the large experimental campaign including 30 tests are presented here (Cf table 3). More details can be obtained in (Di Benedetto H. and Neifar, M., 2000) and (Dongmo-Engeland, 2005). The Table 1 summarized the tests performed; in the details column, the first letter stands for the type of test (Compression or Tension), and the second for the type of solicitation (Cyclic or Static).

Test name	Temperature (°C)	Frequency (Hz)	Mean stress level (MPa)	Compacity	Details
Essai03*	25°C	1 Hz	0.1 MPa		C-C+S
Essai04*	25°C	1 Hz	0.2 MPa		C-C
Essai05*	25°C	1 Hz	0.3 MPa		C-C
Essai06*	25°C	10 Hz	0.1 MPa		C-C
Essai07*	25°C	10 Hz	0.2 MPa		C-C
Essai08*	25°C	10 Hz	0.3 MPa		C-C
Essai09*	35°C	1 Hz	0.1 MPa		C-C
Essai10*	35°C	1 Hz	0.2 MPa		C-C
Essai11*	35°C	10 Hz	0.1 MPa		C-C
Essai12*	35°C	10 Hz	0.2 MPa		C-C
Essai13*	35°C	1 Hz	0.3 MPa		C-C
Essai14*	35°C	10 Hz	0.3 MPa		C-C
Essai15*	15°C	1 Hz	0.1 MPa		C-C
Essai16*	15°C	1 Hz	0.3 MPa		C-C
Essai17*	15°C	10 Hz	0.3 MPa		C-C
Essai18*	15°C	1 Hz	0.2 MPa		C-C
Essai19*	15°C	10 Hz	0.2 MPa		C-C
Essai20*	15°C	10 Hz	0.1 MPa		C-C
Essai21	25°C	1 Hz	0.2 MPa	95.68	C-C
Essai22	25°C	1 Hz	0.2 MPa		C-C
Essai23	25°C	1 Hz	0.1 MPa		C-C
Essai24	25°C	1 Hz	0.2 MPa		C-C
Essai25	25°C		0.2 MPa	94.6	C-S
Essai26	25°C		0.3 MPa	94.9	C-S
Essai27	25°C		0.4 MPa	95.5	C-S
Essai28	25°C		0.4 MPa	95.65	C-S
Essai29	25°C		0.6 MPa	95.42	C-S
Essai30	25°C		0.6 MPa	96.17	C-S
Essai31	25°C		0.6 MPa	94.47	C-S
Essai32	25°C		0.1 MPa	96	T-S
Essai33	35°C	1 Hz	0.05 MPa	94.62	T-C
Essai34	25°C	1 Hz	0.05 MPa	95.24	T-C
Essai35	25°C	10 Hz	0.05 MPa	95.24	T-C
Essai36	25°C	1 Hz	0.1 MPa	95.03	T-C
Essai37	25°C	10 Hz	0.1 MPa	94.6	T-C
Essai38	15°C	1 Hz	0.05 MPa	92.2	T-C
Essai39	15°C	10 Hz	0.05 MPa	95.64	T-C
Essai40	15°C	1 Hz	0.1 MPa	95.02	T-C

Table 1: Test performed. (Di Benedetto H. and Neifar, M., 2000) (*) and (Dongmo-Engeland, 2005).

The load is applied during a time t_1 , then a rest period ($\sigma=0$) is imposed during a time t_2 . This sequence is repeated i times for various t_1 and t_2 (t_{1i} respectively t_{2i}). Chosen t_{1i} times are the following: $t_{11}=35s$; $t_{12}=10s$; $t_{13}=300s$; $t_{14}=1000s$; $t_{15}=3000s$ and $t_{16}=10000s$. The t_{2i} duration is selected long enough in order to obtain of a “quasi” stabilization of permanent deformation. Figure 1 shows the axial deformation obtained for the test “Essai21”.

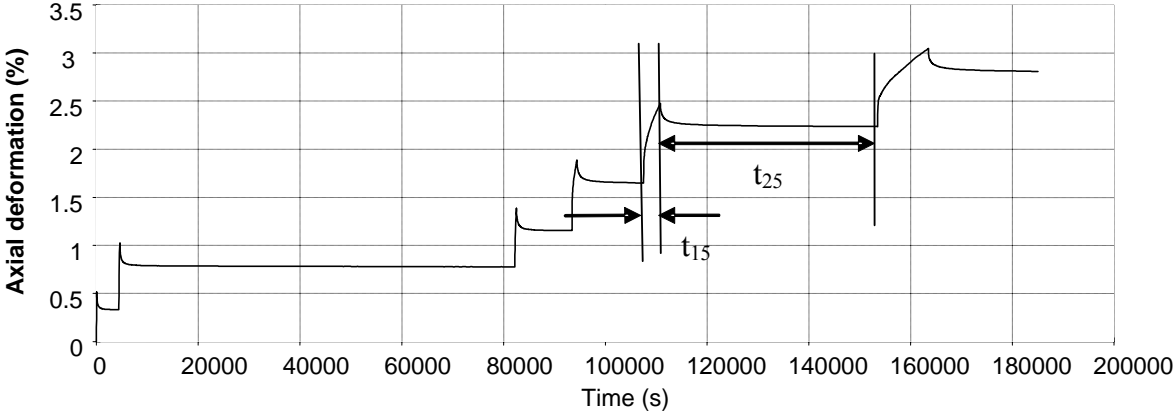


Figure 1: Sequence 5 of the loading protocol and axial deformation for Essai21; $f=1$ Hz, $T=25^\circ C$, $\sigma_{max}=0.4$ Mpa

During loading, the permanent deformation increases with time (or number of cycles) and three phases can be observed for the tests performed in compression as well as the tests performed in extension:

- A first phase with a decreasing rate of permanent deformation.
- A second phase showing a linear evolution of permanent deformation with the number of cycles (constant permanent axial strain rate).
- A third phase with a fast evolution and an increasing rate of permanent axial deformation, which carries out towards the failure.

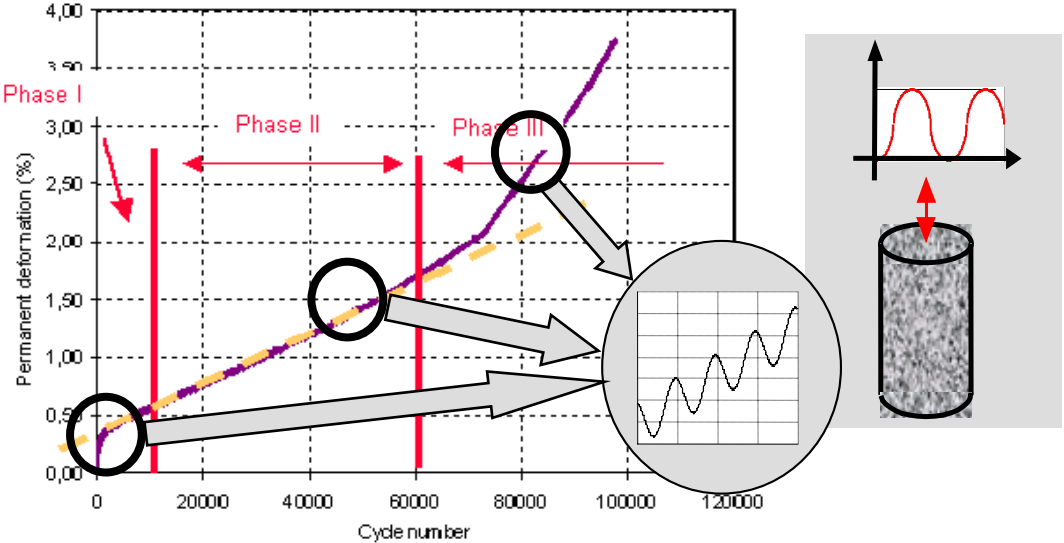


Figure 2: The three stages of the evolution of permanent deformation with the number of cycles for a test performed at $f=10$ Hz, $T=35^\circ C$, $\sigma_{max}=0.4$ Mpa

3 THE “DBN” LAW

One way of modeling the behavior of bituminous mixes consists of using analogical models. A good approximation is obtained by using elementary Kelvin-Voigt (Maxwell) models assembled in series (in parallel) (Mandel, 1966), as shown in Figure 3.

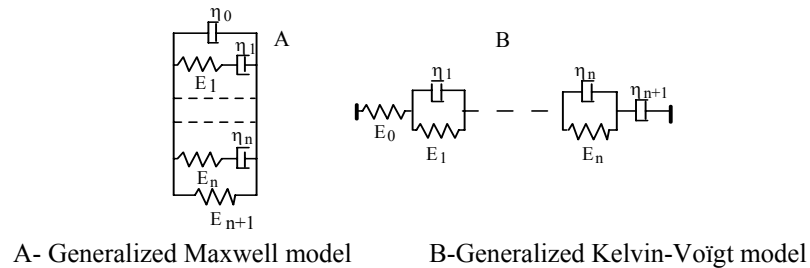


Figure 3: General representation of the linear viscoelastic body (Mandel, 1966), the numbers of elementary bodies can tend toward infinite (continuous spectrum).

Di Benedetto (Di Benedetto, 1987) proposed a generalization of the linear generalized Kelvin Voigt model presented in Figure 3. It is obtained by replacing each dashpot by a purely viscous element “V” and each spring by a non-viscous element “EP” (Figure 4).

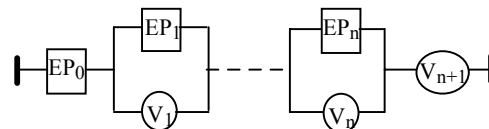


Figure 4: Generalization of the linear viscoelastic body (Cf. Figure 3B) (Di Benedetto, 1987)

3.1 Description of the EP body behavior

The behavior of the EP body is described by a relation between the stress increment ($\Delta\sigma$) and strain increment ($\Delta\varepsilon$) starting from the last point of loading reversal (Figure 5):

$$\Delta\sigma = f(\Delta\varepsilon) \tag{1}$$

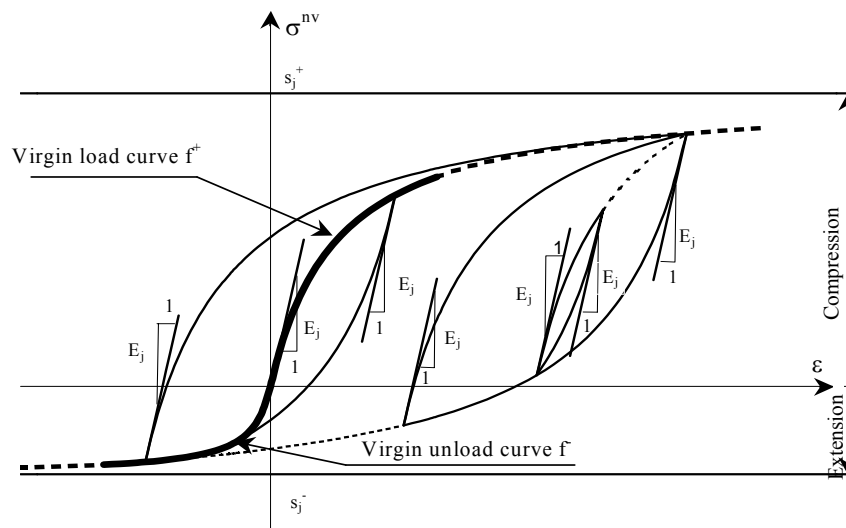


Figure 5: Characterization of the EP_j body behavior, example of cycling sequences.

The function f of the virgin curve has value f^+ with an asymptote s^+ for loading case, and a value f^- with an asymptote s^- for unloading case. s^+ and s^- are the maximum asymptotic of stress, respectively for compression and extension. The function $f^+(f^-)$ is chosen as the hyperbolic function with E_i as initial slope and s^+ (s^-) as asymptotic value.

The general loading and unloading function f is deduced from the function f^+ by applying a cyclic behavior rule which corresponds to an extension of the classical Masing rule (Neifar, 1997).

3.2 Description of the V body behavior

Each V_j body, associated in parallel with the EP_j body, is a dashpot characterized by its viscosity $\eta_j(T)$ which is a function of the temperature (T) that can then be written in the form:

$$\eta_j(T) = \eta_j a_T(T) \quad (2)$$

η_j is the viscosity at the reference temperature T_s . η_j is the viscosity at the reference temperature T_s , and $a_T(T)$ is the shift factor. Considering the WLF equation (Ferry, 1980), it comes:

$$\log(a_T) = \frac{-C_1(T - T_s)}{C_2 + (T - T_s)} \quad (3)$$

Fitting using our data gives: $C_1=23.1$ and $C_2=247.3^\circ\text{K}$ at a reference temperature of $T_s=25^\circ\text{C}$.

3.3 Calibration of the model in the small strains domain

The 2S2P1D model (Olard, 2003), (Di Benedetto et al., 2004), which derived from the Huet-Sayegh model (Sayegh, 1965) has proved to be suitable to represent the linear behaviour of bituminous mixes.

This model has only 7 parameters and its complex modulus is given by the following expression:

$$E^{*2S2P1D}(i\omega\tau) = E(0) + \frac{E(\infty) - E(0)}{1 + \delta(i\omega\tau)^{-k} + (i\omega\tau)^{-h} + (i\omega\beta\tau)^{-1}} \quad (4)$$

The seven constants of this model were obtained from (Di Benedetto H. and Neifar, M., 2000).

The rigidities E_j and the viscosities η_j , of the DBN model, were determined by minimization of the sum of the distances between the complex moduli of the two models (2S2P1D model and “discrete” DBN model) at N points of pulsation ω_j . This minimization is made at the reference temperature ($T_s=23^\circ\text{C}$). We have chosen to use a 15 elements model for our simulations

3.4 Calibration of the model at viscoplastic flow

The criterion used for the viscoplastic flow was proposed by Di Benedetto ((Di Benedetto, 1987), (Di Benedetto and Yan, 1994). We have used the values obtained by Neifar (Neifar, 1997) for our material.

The calibrated model can be used to simulate homogeneous tests. A computer program was developed (Neifar, 1997) allowing to obtain the response for any imposed strain or stress path.

The parameters of the 15 elements model fitted for the tested mix are presented in the table below. It has to be underlines that these 61 parameters are obtained by numerical optimization from 15 constant only. The increase of the number (N) of elementary elements does not increase the number of the constants (15).

Element number	E_j (Mpa)	η_j (Mpa.s)	s_j' (Mpa)	s_j (Mpa)
0	27000			
1	132.00	9737.15	0.69	-0.19
2	459.00	280.82	2.9	-0.81
3	6307.18	280.82	4.01	-1.12
4	6307.18	79.90	5.54	-1.55
5	49716.46	79.90	6.81	-1.91
6	49716.46	79.90	8.22	-2.3
7	57568.94	25.49	9.55	-2.67
8	180103.50	25.49	10.93	-3.06
9	200257.47	25.49	12.28	-3.44
10	203009.78	14.07	13.64	-3.82
11	220257.75	5.06	60.54	-3.82
12	220257.75	5.06	70.91	-3.82
13	220257.75	0.40	79.7	-3.82
14	220257.75	0.40	86.5	-3.82
15	220257.75	0.01	92.91	-3.82

Table 2: Parameters of the DBN law 15 elements

3.5 Simplified version of the DBN law

The computation for a haversine stress loading is extremely time consuming. A simplified version of the law is proposed (Dongmo-Engeland 2005), where the EP_j bodies are replaced by springs which rigidity E_j is the steady-state value of the complex modulus calculated with the loading function f .

We have simulated the evolution of the complex modulus (E^*) (modulus and phase angle) of our mix with the strain amplitude. It has been verified for different conditions of frequencies (0.1; 2.5 and 10HZ), temperatures (5, 23 and 45°C) and imposed stress (0.001, 0.01, 0.05, 0.075, 0.1, 0.2, 0.5 and 1Mpa) that the global and the simplified law give similar results (Figure 6).

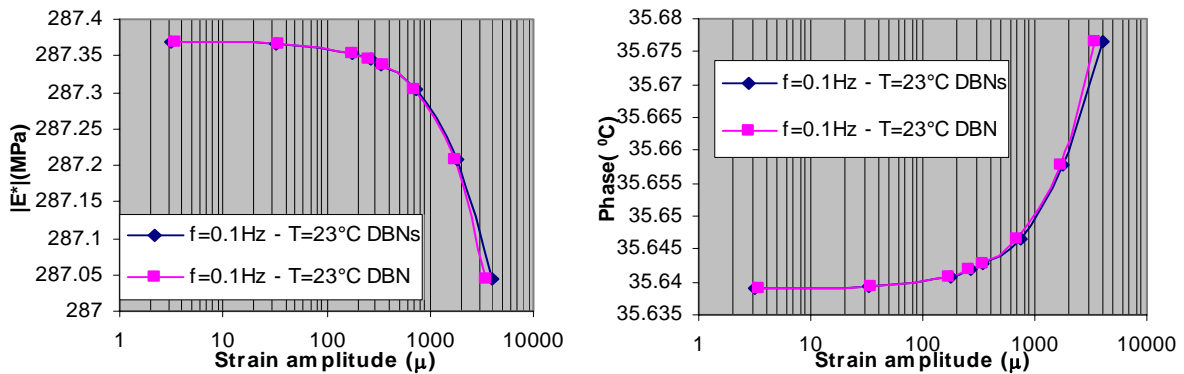


Figure 6: Modulus and phase angle of the complex modulus (E^*) in function of the strain amplitude, calculated with the DBN law and its simplified version (DBNs) for a frequency $f=0.1$ Hz and a temperature $T=23^\circ\text{C}$.

4 INTRODUCTION OF PERMANENT DEFORMATION IN THE DBN LAW

The simplified version of the DBN law is based at each cycle on a “pseudo” viscoelastic calculation. It is therefore necessary to introduce plasticity in this formalism so that at each cycle a small permanent deformation will be accumulated by the model. The developments presented here are valid only for the secondary stage of the development of permanent deformation (Figure 2). The permanent deformation observed in the first stage is taken into account by the EPI bodies of the DBN law. While the rapid deformation increase of stage 3, which is probably more a “boundary” effect than a rheological behavior should be studied separately.

4.1 Cumulative law g.

The accumulated strain at each cycle is the sum of the contribution of each element of the model:

$$\delta\varepsilon_s^p = \sum_{j=1}^{15} \delta\varepsilon_{jmoy}^{perm} \quad (5)$$

It is considered that:

$$\delta\varepsilon_{jmoy}^{perm} = f(\sigma_{jmax}^{nv}) - f(\sigma_{jmin}^{nv}) \quad (6)$$

Where the selected function f is defined by:

$$\left\{ \begin{array}{l} f(\sigma_j^{nv}) = A \frac{S_j^+}{E_j} \left(\frac{\sigma_j^{nv}}{S_j^+} \right)^\beta \text{ if } \sigma_j^{nv} \geq 0 \\ f(\sigma_j^{nv}) = A \frac{S_j^+}{E_j} \left(\frac{\sigma_j^{nv}}{S_j^-} \right)^\beta \text{ if } \sigma_j^{nv} \leq 0 \end{array} \right. \quad (7)$$

It can be observed that the slope of the secondary stage is linked with the distance between the failure stress (si+ or si-) and the highest and the lowest values of the stress when the stabilized cycle is reached ($\sigma_{jmax}^{nv}, \sigma_{jmin}^{nv}$).

5 VALIDATION OF THE MODEL

The formalism introduced to take into account the permanent deformation in the DBN law introduces 2 parameters A and β (equation 7).

A computer program has been developed using the simplified version of the DBN law. It returns the values of the maximum and the minimum stresses of the stabilized cycle for each element ($\sigma_{jmax}^{nv}, \sigma_{jmin}^{nv}$).

The parameters A and β were obtained as the mean values of the better fit for the 30 tests performed. The values obtained are: A = 19.62 and $\beta=3.14$.

The table 3 summarizes the experimental ($\delta\varepsilon_{exp}^p$) and computed values ($\delta\varepsilon_s^p$) of the rate of accumulation of permanent deformation for each cycle during the secondary stage, obtained for the 30 tests. The last 8 tests are performed in extension (tests 33 to 40)

Test number	$\delta\varepsilon_{\text{exp}}^{\text{P}}(\%)$	$\delta\varepsilon_{\text{s}}^{\text{P}}(\%)$	Error	Relative error(%)
3	3.19E-06	3.03E-06	0.05	4.95
4	3.10E-05	4.79E-05	0.54	54.28
5	3.59E-04	1.74E-04	0.52	51.57
6	1.01E-06	4.70E-07	0.53	53.28
7	7.31E-06	6.58E-06	0.10	9.99
8	2.31E-05	2.21E-05	0.04	4.42
9	8.94E-05	3.51E-05	0.61	60.71
10	4.07E-04	2.22E-04	0.45	45.45
11	3.50E-06	2.46E-06	0.30	29.74
12	2.27E-05	2.21E-05	0.03	2.68
13	1.25E-03	7.79E-04	0.38	37.80
14	8.71E-05	8.07E-05	0.07	7.38
15	5.80E-07	6.81E-07	0.17	17.49
16	2.16E-05	2.05E-05	0.05	4.81
17	2.24E-06	2.07E-06	0.08	7.61
18	1.80E-05	5.91E-06	0.67	67.14
19	1.57E-06	7.26E-07	0.54	53.86
20	1.07E-06	6.55E-08	0.94	93.88
21	4.50E-05	4.81E-05	0.07	6.95
22	3.29E-05	4.94E-05	0.50	50.12
23	1.27E-05	5.54E-06	0.56	56.30
24	2.31E-04	6.54E-05	0.72	71.69
33	-2.34E-03	-1.68E-04	0.93	92.84
34	-1.29E-04	-3.57E-05	0.72	72.34
35	-9.13E-06	-3.32E-06	0.64	63.57
36	-1.89E-03	-3.19E-04	0.83	83.11
37	-1.16E-04	-2.94E-05	0.75	74.69
38	-3.56E-05	-5.24E-06	0.85	85.27
39	-7.41E-07	-8.73E-07	0.18	17.81
40	-4.49E-05	-4.69E-05	0.04	4.44

Table 3: Experimental and computed values of the permanent deformation rate of accumulation during the secondary stage, obtained for the 30 tests.

It is seen that 5 tests out of 30 seems to be outliers with this formalism (tests 20, 33, 36, 37 and 38), among which 4 are performed in extension. Knowing that the tests in extension were practically hard to perform correctly, given how fast the deformations occurs. It is an encouraging result for the proposed model.

Figures 7 to 9 present a graphic comparison between the experimental and computed values of the permanent deformation rate of accumulation, which are looked here as the experimental and computed slopes (E slope and S slope) obtained during the secondary stage. ε axial, ε_e and ε_p are respectively the axial deformation obtained during the test, the reversible and the permanent deformation computed using the DBN law.

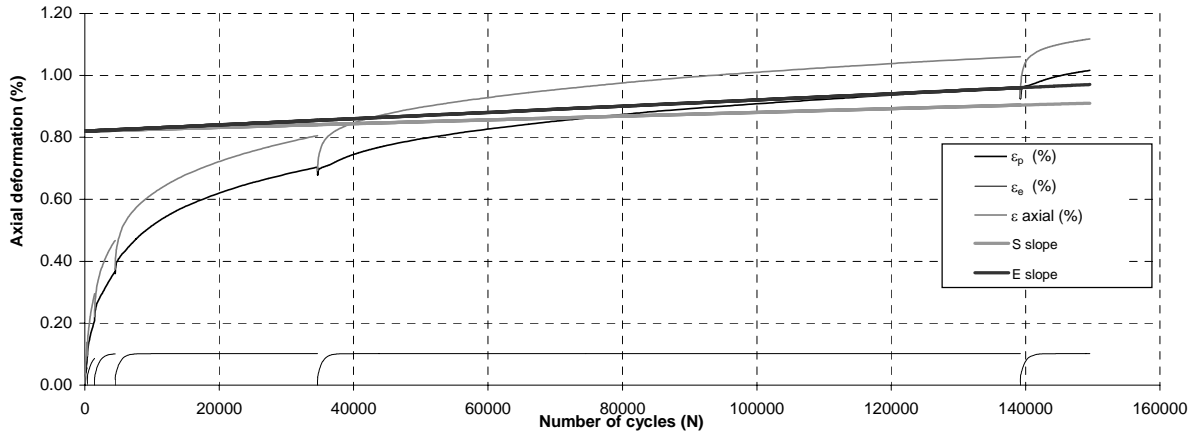


Figure 7: Experimental and computed strain rate accumulation, test 6; $f=10$ Hz, $T=25^\circ\text{C}$, $\sigma_{\max}=0.2$ Mpa (Dongmo-England, 2005).

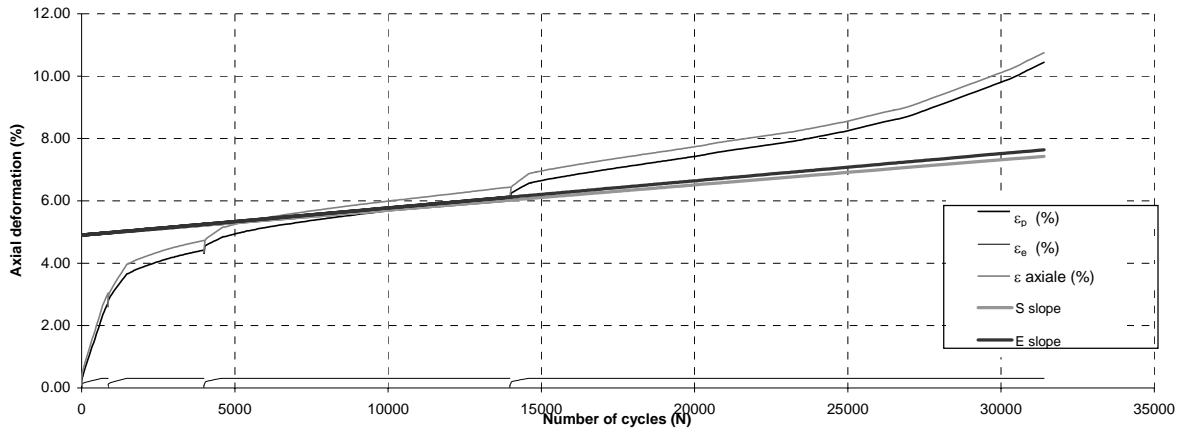


Figure 8: Experimental and computed strain rate accumulation, test 14; $f=10$ Hz, $T=35^\circ\text{C}$, $\sigma_{\max}=0.6$ Mpa (Dongmo-England, 2005).

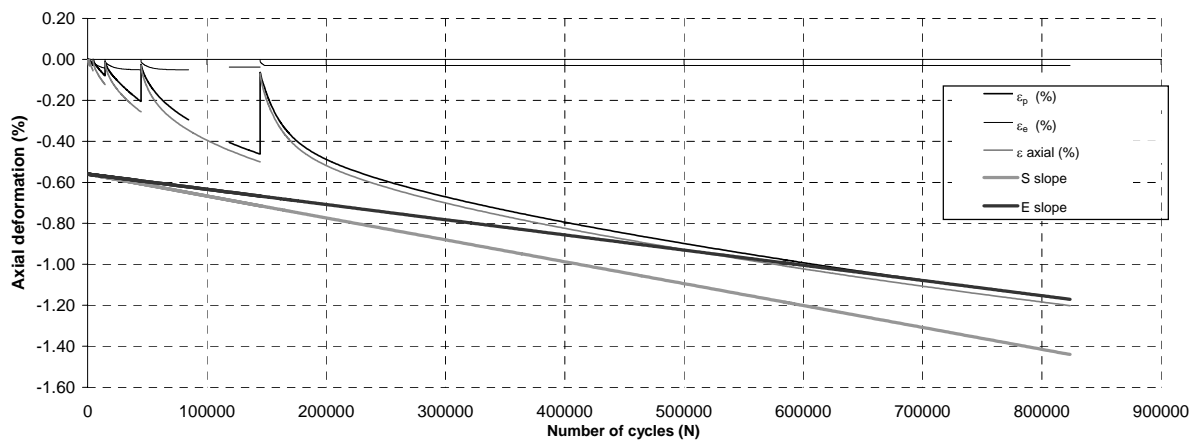


Figure 9: Experimental and computed strain rate accumulation, test 39; $f=10$ Hz, $T=15^\circ\text{C}$, $\sigma_{\max}=0.6$ Mpa (Dongmo-England, 2005).

6 CONCLUSION

We have proposed an improvement to the rheological model developed at the DGCB for bituminous mixes, which allow taking into account permanent deformation due to cyclic effects (creating rutting).

A new homogeneous test has been developed at the DGCB, specifically designed to study permanent deformation of bituminous mixes. We have used the results of 30 tests performed with this apparatus to calibrate the proposed cumulative law.

It is seen that the proposed formalism gives encouraging results for the simulation of the rate of accumulation of permanent deformation during the secondary stage of the tests.

REFERENCES

- Di Benedetto H. and Neifar, M. , Novembre 2000. *Etude de l'orniérage des mélanges bitumineux : mise au point d'un dispositif expérimental et campagne d'essais*. Rapport de synthèse du contrat LCPC n° 97/259. ENTPE-DGCB. 60 p.
- Di Benedetto, H., Dongmo B., Neifar, M., 2003. *Permanent deformation and complex modulus: Two different characteristics from a unique test*. 6th International RILEM Symposium on Performance Testing and Evaluation of Bituminous Materials (PTEBM '03), Zurich, Switzerland.
- Dongmo-Engeland B., 2005. *Caractérisation des déformations d'orniérage des chaussées bitumineuses*. Thèse de Doctorat ENTPE-INSA.
- Mandel, J., 1966. *Cours de Mécanique des Milieux Continus*. Paris: Edition Gauthier-Villars. Tome I et II, 848 p.
- Di Benedetto, H., 1987. *Modélisation du comportement des géomatériaux: Application aux enrobés bitumineux et aux bitumes*. Thèse d'Etat : Institut National Polytechnique de Grenoble. 252 p.
- Neifar, M., 1997. *Comportement thermomécanique des enrobés bitumineux : Expérimentation et modélisation*. Thèse de Doctorat ENTPE-INSA.
- Ferry, J.D., 1980. *Viscoelastic properties of polymers*. New York : ed. J.W. Sons, 641 p.
- Olard, F., 2003. *Comportement thermomécanique des enrobés bitumineux à basse température. Relations entre les propriétés du liant et de l'enrobé*. Thèse de Doctorat ENTPE-INSA.
- DI BENEDETTO, H., OLARD, F., SAUZEAT, C., and DELAPORTE, B., 2004. *Linear viscoelastic behavior of bituminous materials : from binders to mixes*, EATA Nottingham, International Journal of Road Materials and Pavement Design, Vol.5, Special Issue, pp. 163-202.
- Sayegh, G., 1965. *Variation des modules de quelques bitumes purs et bétons bitumineux*. Thèse de Doctorat Ingénieur : Faculté des Sciences de l'université de Paris. 74 p.
- Di Benedetto, H. and Yan, X., 1994. *Comportement mécanique des enrobés bitumineux et modélisation de la contrainte maximale*. Materials and structures, N° 21, p 539-47.